Improving the accuracy of musculotendon models for the simulation of active lengthening

Matthew Millard[A,B,C] , Fabian Kempter[B] ,Norman Stutzig[A], Tobias Siebert[A,C], and Jörg Fehr[B,C]

Abstract Vehicle accidents can cause neck injuries which are costly for individuals and society. Safety systems could be designed to reduce the risk of neck injury if it were possible to accurately simulate the tissue-level injuries that later lead to chronic pain. During a crash, reflexes cause the muscles of the neck to be actively lengthened. Although the muscles of the neck are often only mildly injured, the forces developed by the neck's musculature affect the tissues that are more severely injured. In this work, we compare the forces developed by MAT_156, LS-DYNA's Hill-type model, and the newly proposed VEXAT muscle model during active lengthening. The results show that Hill-type muscle models underestimate forces developed during active lengthening, while the VEXAT model can more faithfully reproduce experimental measurements.

Keywords active lengthening, muscle model, neck injury, titin, active human body model

I. INTRODUCTION

Vehicle accidents often cause neck injuries [1] [2] that are costly to treat [3] and are difficult to predict using computer simulation [4] [5]. There is clinical evidence that people who suffer from chronic pain as a result of neck injury have sustained injuries to the facet joint capsules, the ligaments of the neck, intervertebral disks, and cervical vertebrae [6]. The musculature of the neck is important to accurately simulate because the tension developed by the neck's muscles directly affects the stresses and strains of the tissues that are injured.

Experimental measurements of the kinematics and muscle activity during whiplash show that many of the neck's muscles are actively lengthened throughout a crash [7] [8]. When an active muscle is forcibly lengthened, it can develop tensions that greatly exceed the maximum isometric force (f_o^M) of the muscle [9] [10] right up until the muscle is injured [11] and ruptures at its failure force (f_F^M, 3.41 ± 0.33 f_o^M). Most of this tension is developed, particularly at long lengths [12] [13], by the semi-active titin filament [14] [15]. Hill-type muscle models [16] [17] are often used to simulate the musculotendon forces acting on human body models (HBMs) in FE simulations [18] [19] [20]. Hill-type muscle models lack a titin element since the formulation was developed decades [21] [22] [23] prior to the discovery of titin [14] [15][2].

In this work, we simulate two active-lengthening experiments [9] [24] and compare the accuracy of the force response of LS-DYNA's MAT_156 [18] to our LS-DYNA implementation of the VEXAT muscle model [25]. The VEXAT model [25] extends prior work that includes titin [26] [27] [28] by adding additional mechanical detail relevant to injury prediction — such as a viscoelastic cross-bridge and tendon element — using only a few states beyond that of a conventional Hill-type model. First, we simulate the in-situ experiments of Herzog and Leonard [9] to directly compare the response of both models to the response of biological muscle. Next, we simulate a more aggressive active lengthening that takes each model through the various force thresholds of muscular injury [11]: mild injury (2.39 f_o^M or 70% f_F^M), major injury (3.07 f_o^M or 90% f_F^M), and finally rupture (3.41 f_o^M). The results of the Herzog and Leonard [9] simulation will show how accurately these two models are able to simulate modest active lengthening in comparison to biological muscle, while the response to aggressive lengthening will illustrate what can be expected during a more extreme event such as a crash simulation.

[1] M.Millard (+49 711 685 51763, matthew.millard@inspo.uni-stuttgart.de) is a Postdoctoral Researcher, F.Kempter is a Research Associate and Doctoral Student, N.Stutzig is a Privatdozent, T.Siebert is a Professor, and J.Fehr is a Professor. The authors work at the [A]Institute for Sport and Movement Science, [B]Institute of Engineering and Computational Mechanics, and the [C]Stuttgart Center of Simulation Science at the University of Stuttgart, Stuttgart, Germany.

[2] Titin is known as connectin in Japan, where it was first discovered by Maruyama [14]

II. METHODS

A muscle model is defined by the experiments that it can replicate and the mechanisms that it embodies. Hill-type muscle models are phenomenological models because the formulation makes direct use of experimentally measured relationships without modelling the underlying processes. The tension (f^M) developed by the contractile element (CE) of LS-DYNA's MAT_156 [18] (Fig. 1A) is given by the product of the activation state of the muscle (a, which ranges between 0-1), the active-force-length relation ($\mathbf{f^L}(\ell^M)$), and the force-velocity relation ($\mathbf{f^V}(v^M)$)

$$f^M = f_o^M(a\, \mathbf{f^L}(\ell^M)\, \mathbf{f^V}(v^M) + \mathbf{f^{PE}}(\ell^M)) \quad (1)$$

all of which is added to the elastic force developed by the parallel element ($\mathbf{f^{PE}}(\ell^M)$) (Fig. 1B). By construction, the Hill model can reproduce Hill's iconic force-velocity curve [21] during active shortening (concentric contraction). In addition, the model can also reproduce the passive [29] and active [30] isometric force-length relations. The MAT_156 implementation is stateless because it lacks activation dynamics and does not include an elastic tendon [18]. While the FE model can be edited to add an elastic tendon segment in series with a MAT_156 element, care must be taken to ensure that the tendon properties scale with the f_o^M of the corresponding CE [31].

The VEXAT model [25](Fig. 1C) includes additional detail that is missing from Hill-type muscle models in general and the MAT_156 specifically (Fig. 1A). The VEXAT model derives its name from the lumped viscoelastic (VE) cross-bridge (X) and active-titin (AT) elements that it contains. The additional mechanical detail of the VEXAT model comes at the cost of five states to simulate activation dynamics (a), the position and velocity of the point of attachment of the lumped cross-bridge (XE) to actin (ℓ^S and v^S), the length of the CE (ℓ^M), and the position of the titin-actin bond (ℓ^1). The extra detail allows the active force developed by the CE (Fig. 1D),

$$f^M = f_o^M(a\, \mathbf{f^L}(\ell^S + \mathrm{L}^M)(k_o^X\, \ell^X + \beta_o^X v^X) + \mathbf{f^2}(\ell^2) + \mathbf{f^{ECM}}(\ell^{ECM}) + \beta^\varepsilon v^M - \mathbf{f^{KE}}(\ell^M)/\cos\alpha) \quad (2)$$

to be described in terms of the elastic ($k_o^X\, \ell^X$) and damping ($\beta_o^X v^X$) forces developed by the XE scaled by the proportion of attached cross-bridges ($a\, \mathbf{f^L}(\ell^S + \mathrm{L}^M)$) of the model. The CE's passive forces come from the extracellular matrix ($\mathbf{f^{ECM}}(\ell^{ECM})$) and a mixture of active and passive forces from the distal segment of the titin model ($\mathbf{f^2}(\ell^2)$). The remaining two terms ensure that the model is stable during simulation ($\beta^\varepsilon v^M$) and cannot reach unrealistically short lengths ($\mathbf{f^{KE}}(\ell^M)/\cos\alpha$). The tension developed by the CE acts at a pennation angle α to the viscoelastic tendon (Fig. 1C and 1D). The pennation angle α is constrained to follow a specific length-angle relation in an effort to mimic the constant volume property of muscle [32]. As is typical [16], we assume that the muscle volume has a fixed thickness and a cross-section that is described by a constant height (h) parallelogram where $\ell^M \sin\alpha = h$. While the VEXAT model may seem to only apply to a sarcomere (the smallest contractile element of a muscle which is 2.73 µm long in humans), this model can be applied to whole muscle because the mechanical properties of sarcomeres scale with size: f_o^M scales with cross-sectional area [33], $\mathbf{f^L}(\ell^M)$ scales with length [34], the maximum shortening velocity scales with length [35], and titin's passive properties also scale with length [36] [37]. This model is both a mechanistic model and a phenomenological model in classification because it includes additional mechanical detail and yet still relies on phenomenological characteristics to drive the XE attachment point over time [25].

The active forces developed by titin, however, are not driven to follow any prescribed phenomena. To reduce the computational cost of simulating titin, the VEXAT model [25] treats titin as a two-segmented spring: the first spring spans a distance ℓ^1 from near the Z-line to the bond location within the titin element, while the second spring spans a distance ℓ^2 from the bond location to the myosin tip. Upon activation, damping forces are applied between the actin element and the point between the ℓ^1 and ℓ^2 segments. When titin is bound to actin, the ℓ^2 element bares nearly all the strain, roughly doubling titin's stiffness compared to when the CE is passive. This modelling change leads to an important difference between the two models: the Hill model treats the active force response of muscle to lengthening as a velocity-dependent phenomenon, while the VEXAT model [25] treats this same process as both velocity and displacement-dependent phenomena.

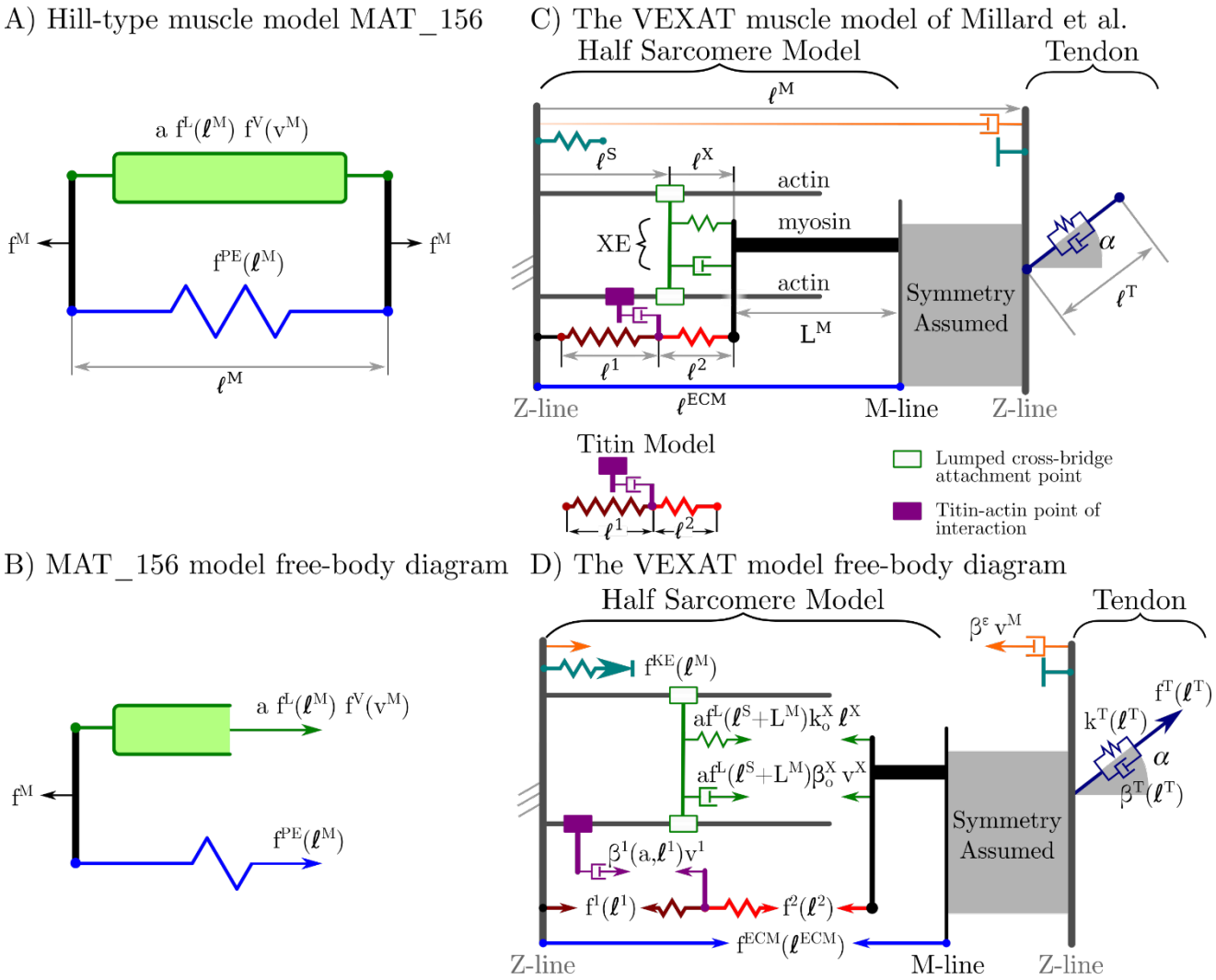

Fig. 1. LS-DYNA's Hill-type muscle model MAT 156 (A.) consists of an active element (green) in parallel with a passive element (blue) (B.). We have implemented the VEXAT (C.) model [25][3] as a material in LS-DYNA. The VEXAT model's active components include a lumped viscoelastic cross-bridge (green) a semi-active titin element, and numerical damping (orange) (D.). The passive elastic components of the VEXAT model include an elastic extracellular matrix ECM, a viscoelastic tendon (dark blue), and a small compressive element (blue-green) that prevents the contractile element (CE) from approaching unrealistically short lengths (D.). Upon activation, the damping forces (purple) slow the ℓ^1 element, and the ℓ^2 segment stretches (D.). Rigid components appear in black or dark grey, while the force-generating elements are illustrated in colour.

To fairly evaluate the two models, we have fitted the models to be as similar as possible to the cat soleus used in the experiments of Herzog and Leonard [9]. First, we have set the values of the optimal fibre length (ℓ_o^M) and f_o^M of MAT_156 to be identical to the values produced by the VEXAT model when it is evaluated along the length of the tendon as shown in Table 1 (Appendix A). Since the VEXAT model includes a constant height pennation model [25], these properties differ slightly as the length and angle of the VEXAT's CE change with respect to the direction of the tendon. These differences are small because the fibres of a cat soleus are only pennated by 7°. Next, we have set the active-force-length and passive-force-length curves to fit the data of Herzog and Leonard [9] and to be identical when the VEXAT model is evaluated in the direction of the CE (Fig. 2A). The passive force-length curves of the two models match if the CE is passive: as soon as the CE is active, the point between the ℓ^1 and ℓ^2 segments of the titin model viscously bond to actin and the stiffness of the titin filament and ECM together roughly doubles (Fig. 2A, magenta line). The curves that represent the passive force-length curves in MAT_156 and the ECM curves in VEXAT become linear when stretched sufficiently, as is typical

[3] The images of the VEXAT model [25] have been used under the terms of the CC-BY license3 and have been modified from the original form. The images in this figure are also licensed under the terms of the CC-BY licence3. A copy of the license can be found at https://creativecommons.org/licenses/by/4.0/legalcode

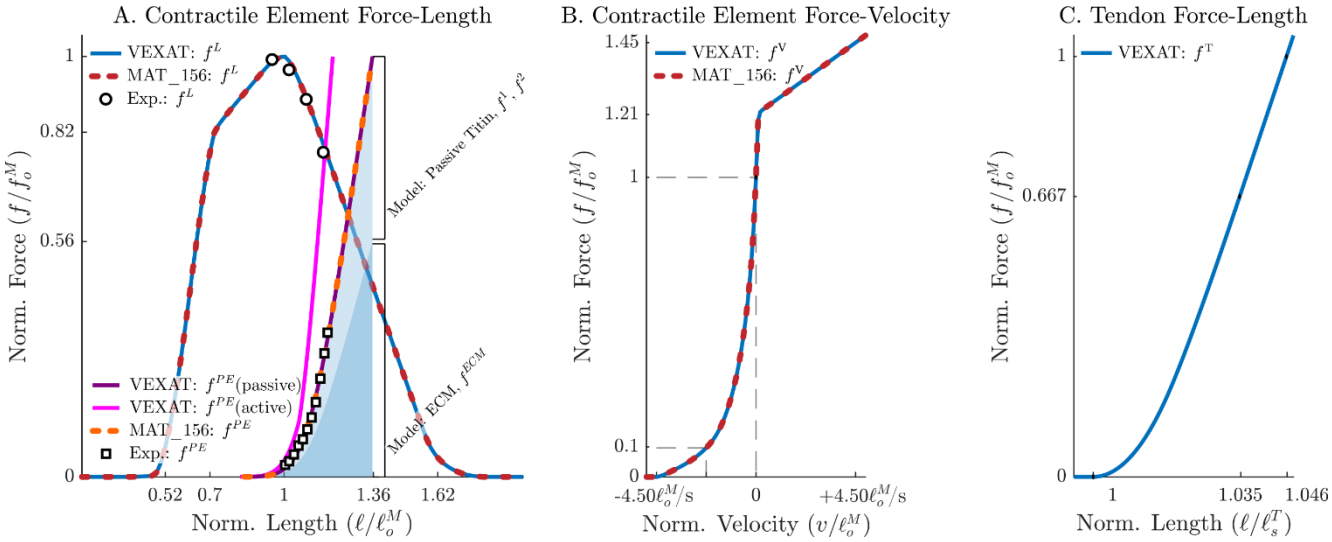

Fig. 2. The active and passive force-length curves (A) of the two models fit the data of Herzog and Leonard [9] and are identical when the VEXAT model is evaluated in the direction of the CE. The passive force-length curve of the VEXAT model is formed by a nearly equal contribution from the ECM and the titin element. When the CE is activated, the stiffness of titin increases and the force produced by the ECM and titin roughly doubles (magenta line). Both models have the same force-velocity curve (B) that fits the data of Scott et al. [38] during shortening and have been adjusted to fit the data of Herzog and Leonard [9] during lengthening. The VEXAT model includes a viscoelastic tendon (C), which has a nonlinear curve that fits the data from Scott et al. [39].

of skeletal muscle [40] [41]. Similarly, the force-length curves of titin's segments become linear at large strains, as indicated by the sarcomere-level experiments of Leonard et al. [12], even though this differs from a popular theoretical model (worm-like-chain model) of titin's force-length curve [42]. The bond location within the VEXAT's titin element has been chosen to fit the data of Herzog and Leonard [9]. Finally, Scott et al.'s measurements [38] have been used to fit the shortening side of the force-velocity curve, while the lengthening side of the curve has been fit to the data of Herzog and Leonard [9].

We first evaluate the models by comparing the peak forces developed during the active lengthening phase to the experimental data of Herzog and Leonard [9]. Next, we compare the root-mean-squared-error (RMSE) between each of the models and the experimental measurements during the active-lengthening phase of the experiment [9]. Although the experiment includes other phases, the active-lengthening phase has the largest forces and is thus the most relevant to the simulation of injury. In the second simulation, we evaluate the length change that each model must undergo to reach the threshold of minor injury since clinical evidence [6] suggests that minor injury to the neck muscles is commonly caused by whiplash.

III. RESULTS

The VEXAT model has an active lengthening force profile (Fig. 3A) that closely matches the data of Herzog and Leonard [9] both in peak value (35.7N vs 36.6N) and form (RMSE 0.8N) during the active lengthening phase between times 2.39s-3.39s (Fig. 3B) of the experiment. Although MAT_156 does develop enhanced forces during the active lengthening experiment, the peak forces are smaller than the experimental data (27.3 N vs 36.6 N), deviate from the experimental data (RMSE 4.7N), and are immediately reduced following the end of the ramp. In the normalised force-length space (Fig. 3C), it is clear that both the experimental data [9] and the VEXAT model develop active forces that grow in magnitude relative to the sum of the active and passive force-length curves (grey line). In contrast, the active force developed by the Hill model drops as the CE is lengthened further down the descending limb of the active force-length curve and will approach zero as the ℓ^M exceeds 1.62 ℓ_o^M (Fig. 2A).

The tension developed by the VEXAT model increases faster than MAT_156 (Fig. 4A) if the ramp length is

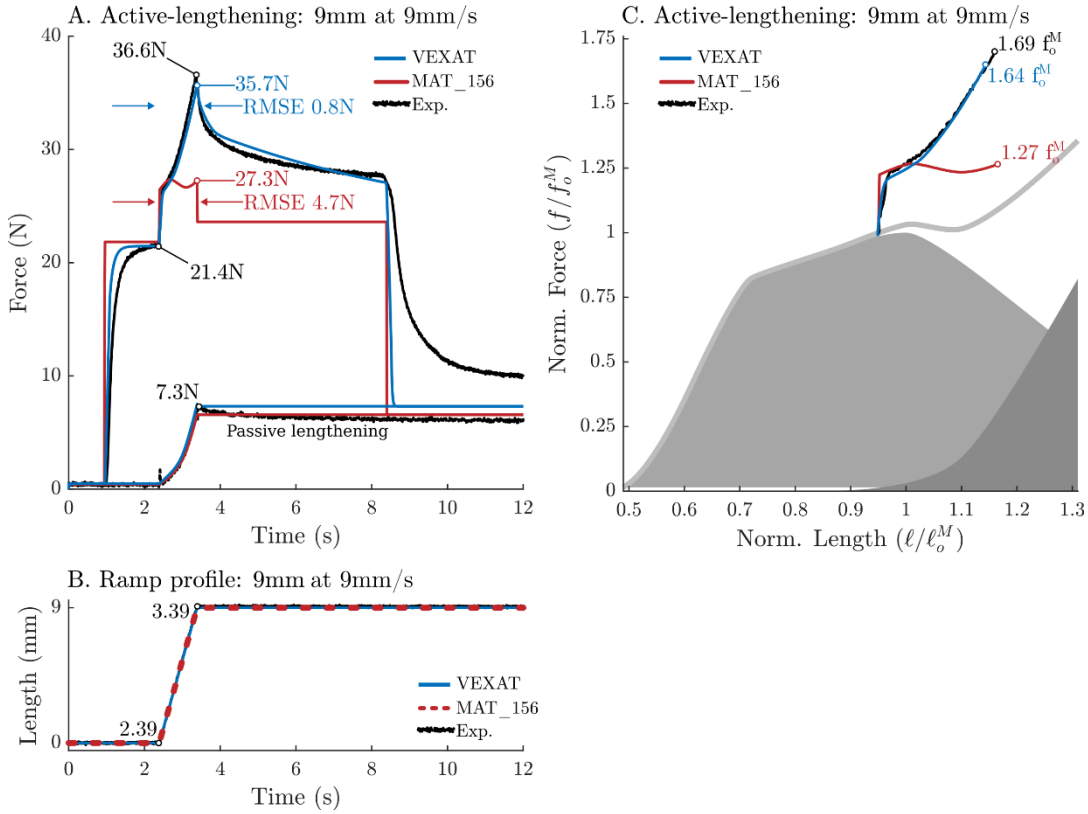

Fig. 3. During active lengthening, both the experimental data (Exp.) of Herzog and Leonard [9] and the VEXAT model develop a tension that increases as the muscle is lengthened (A). While the tension of the MAT_156 model does increase, it is short-lived and smaller in magnitude than the experimental data. The small differences that arise during the passive lengthening of the two models (A) are due to the elastic tendon of the VEXAT model and the pennation model, two components that MAT_156 lacks. The ramp-length change forced the models through a 9mm extension at a constant rate of 9mm/s (B). The tensions developed in the experiment and by the VEXAT model grow faster than the boundary formed by the active and passive-force length curves (C, grey line). The MAT_156 approaches the passive force-length curve as the contribution from the active-force-length curve decreases.

increased to 52 mm (Fig. 4B). As a result, the VEXAT model crosses the active minor injury force threshold of 2.39 f_o^M [11] at a normalised length of 1.34 ℓ_o^M, while the MAT_156 does not reach this threshold until the normalised length of 1.71 ℓ_o^M (Fig. 4). The difference in normalised length between the two models at the threshold for minor injury (0.37 ℓ_o^M) is similar at the thresholds for major injury (0.35 ℓ_o^M), and rupture (0.35 ℓ_o^M) (Fig. 4).

IV. Discussion

Neck injuries sustained during vehicle accidents are common but perhaps could be prevented if it were possible to simulate the tissue-level injuries that lead to chronic pain. Great progress has been made in developing anatomically detailed male and female FE HBM models [4] [5], though Hill-type muscle models have been used to represent the musculature of the neck. Hill-type muscle models are not able to develop the large forces observed when biological muscle is actively lengthened. Since the muscles of the neck are known to be actively lengthened during whiplash [7] [8], we have compared in-situ experimental recordings of actively lengthened muscles to the simulated response of LS-DYNA's Hill-type muscle model (MAT_156) to the responses of the VEXAT model [25]. In contrast to MAT_156, the VEXAT model [25] includes a titin filament which produces enhanced forces during active lengthening [12] [13].

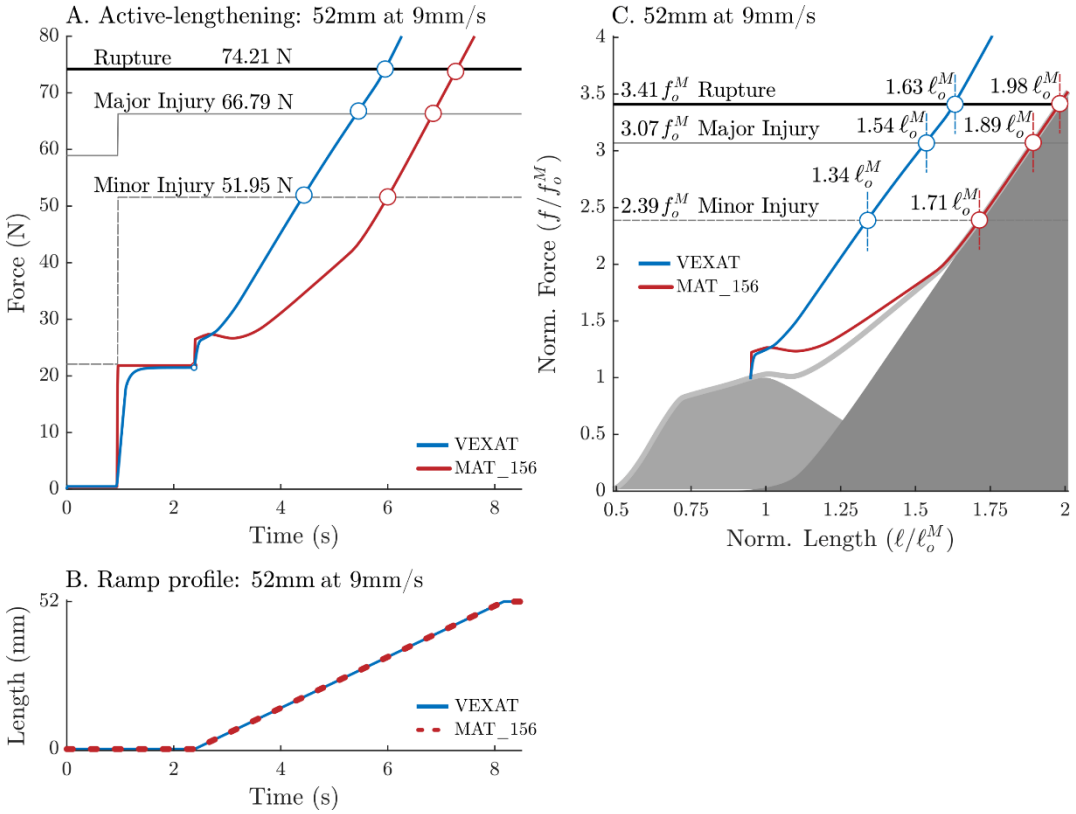

Fig. 4. Both the VEXAT and MAT_156 models develop forces that are large enough to pass through the active thresholds for minor injury, major injury, and rupture (A) when the ramp is extended from 9 mm to 52 mm (B). In a normalised force-length space (C), the VEXAT model passes through the thresholds for injury at shorter lengths than the MAT_156 model. This has implications for simulating whiplash: a muscle that is able to develop high forces at lower strains will reduce the amount of resulting head movement and will apply larger forces to the structures of the neck.

In our simulations of an in-situ active lengthening experiment, the VEXAT muscle produced force responses that more faithfully followed the experimental measurements than MAT_156 (Fig. 3). Unfortunately, we do not have experimental data that we can use to assess the accuracy of the aggressive active-lengthening injury simulation (Fig. 4), though our results highlight meaningful differences between the two models. While there are excellent lengthening injury datasets in the literature [24] [43], neither of these datasets contains the additional information that is required to fit the models to the specimen so that an accurate simulation of the experiment can be performed. Since titin has been shown to be capable of developing large forces in actively lengthened sarcomeres [12], we expect that the VEXAT model will produce more accurate results than a Hill-type model during the active lengthening that takes place during whiplash. While we hope to achieve improved accuracy during simulations of whiplash by including titin in the muscle model, other strategies have also been taken.

Biologically inspired controllers and Hill-type models have been used to improve the accuracy of simulated head and neck movement during whiplash. Models of the vestibulocollic and cervicocollic reflexes [44] [45], as well as stretch reflexes [46] [47], have improved the accuracy of head and neck models driven by Hill-type muscle models. More advanced Hill-type models than MAT_156 have also been developed to improve the response of the head and neck to sudden accelerations. The Hill-type model of Kleinbach et al. [19] [20] includes a more detailed activation dynamic and force-length model than is typical and was used to simulate the response of head movement to a sudden 1g acceleration [48]. Happee et al.'s [45] Hill-type model has been used to simulate the response of the head to vibration and to a sudden 15g acceleration [49]. While each of these works [44] [45] [46] [47] has shown improved results through the use of a biologically inspired controller, the results of these works are likely affected, to some degree, by the inaccurate force development of the underlying Hill-type model during active lengthening.

We have shown that a Hill-type muscle can underestimate the peak force developed by biological muscle by as much as 25% during an active lengthening experiment [9] with a modest 20% strain. Since mild muscle injury is often reported following whiplash [6], it is possible that Hill-type models are greatly underestimating the forces

applied by the neck muscles during simulations of whiplash. We plan to continue this work to see how these models affect the kinematics, internal loads, and risk of injury during simulations of whiplash.

V. CONCLUSIONS

We found that the VEXAT model [25] can more accurately capture the force development of modestly actively lengthened muscle than the MAT_156 Hill-type muscle model when compared to the experiments of Herzog and Leonard [9]. The differences between the VEXAT and Hill-type muscle models are even more pronounced when the models are actively lengthened to the point of mild injury: the VEXAT model reaches the force threshold for mild injury at lengths 0.35 ℓ_o^M shorter than in the Hill-type model. Taken together, it is likely that the Hill-type muscle models used in simulations of car accidents have been underestimating the amount of force the musculature of the neck applies to the cervical spine.

VI. ACKNOWLEDGEMENT

Funded by Deutsche Forschungsgemeinschaft (DFG, German Research Foundation) under Germany's Excellence Strategy - EXC 2075 – 390740016. We acknowledge the support of the Stuttgart Center for Simulation Science (SimTech).

VII. REFERENCES

[1] Galasko CSB, Murray PM, et al. Neck sprains after road traffic accidents: a modern epidemic, *Injury,*1993, 24(3): 155–157

[2] Richter M, Otte D, Pohlemann T, Krettek C, Blauth M. Whiplash-type neck distortion in restrained car drivers: frequency, causes and long-term results, *European Spine Journal,* 2000, 9: 109–117.

[3] Carlsson I, Hedin M, et al. The whiplash commission final report, Klara Norra kyrkogata 33, 111 22 Stockholm, 2005.

[4] John J, Klug C, Kranjec M, Svenning E, Iraeus J. Hello, world! VIVA+: A human body model lineup to evaluate sex-differences in crash protection, *Frontiers in bioengineering and biotechnology,* 2022, 10: 1-19.

[5] Schwartz D, Guleyupoglu B, Koya B, Stitzel JD, Gayzik FS. Development of a computationally efficient full human body finite element model, *Traffic injury prevention,* 2015, 16: S49–S56.

[6] Siegmund GP, Winkelstein BA, Ivancic PC, Svensson MY, Vasavada A. The anatomy and biomechanics of acute and chronic whiplash injury, *Traffic injury prevention,* 2009, 10(2): 101–112.

[7] Brault JR, Siegmund GP and Wheeler JB. Cervical muscle response during whiplash: evidence of a lengthening muscle contraction, *Clinical biomechanics,* 2000, 15(6): 426–435.

[8] Vasavada A, Brault JR and Siegmund GP. Musculotendon and fascicle strains in anterior and posterior neck muscles during whiplash injury, *Spine,* 2007, 32(7): 756–765.

[9] Herzog W, Leonard TR. Force enhancement following stretching of skeletal muscle: a new mechanism, *The Journal of Experimental Biology,* 2002, 205(9): 1275–1283.

[10] Siebert T, Leichsenring K, et al. Three-dimensional muscle architecture and comprehensive dynamic properties of rabbit gastrocnemius, plantaris and soleus: input for simulation studies, *PLoS one,* 2015, 10(6): e0130985.

[11] Nölle LV, Mishra A, Martynenko OV and Schmitt S. Evaluation of muscle strain injury severity in active human body models, *Journal of the mechanical behavior of biomedical materials,* 2022, 135: 105463.

[12] Leonard TR, Joumaa V, Herzog W. An activatable molecular spring reduces muscle tearing during extreme stretching, *Journal of biomechanics,* 2010, 43(15): 3063–3066.

[13] Tomalka A, Rode C, Schumacher J, Siebert T. The active force–length relationship is invisible during extensive eccentric contractions in skinned skeletal muscle fibres, *Proceedings of the Royal Society B: Biological Sciences,* 2017, 284(1854): 20162497.

[14] Maruyama K. Connectin, an elastic protein from myofibrils, *The Journal of Biochemistry,* 1976, 80(2): 405–407.

[15] Wang K, McClure J and Tu ANN. Titin: major myofibrillar components of striated muscle, *Proceedings of the National Academy of Sciences,* 1979, 76(8): 3698–3702.

[16] Zajac FE. Muscle and tendon: Properties, models, scaling, and application to biomechanics and motor control, *Critical Reviews in Biomedical Engineering,* 1989, 17(4): 359–411.

[17] Jin Z, Li J, Chen Z, editors. Computational modelling of biomechanics and biotribology in the musculoskeletal system: biomaterials and tissues, 173-204, *Woodhead Publishing*, Duxford, United Kingdom, 2020.

[18] Gladman B, LS-DYNA Keyword User's Manual: Volume II Material Models, 2-792 - 2-795, 2-1382 - 2-1386, Livermore Software Technology Corporation, Livermore, United States of America, 2016.

[19] Kleinbach C, Martynenko O, et al. Implementation and validation of the extended Hill-type muscle model with robust routing capabilities in LS-DYNA for active human body models, *Biomedical engineering online,* 2017, 16:1–28.

[20] Haeufle DFB, Günther M, Bayer A, Schmitt S. Hill-type muscle model with serial damping and eccentric force–velocity relation, *Journal of biomechanics,* 2014, 47(6): 1531–1536.

[21] Hill AV. The heat of shortening and the dynamics constants of muscle, in *Proceedings of the Royal Society of London*, 1938, 126(843): 136-195.

[22] Wilkie DR. The mechanical properties of muscle, *British medical bulletin,* 1956, 12(3): 177–182.

[23] Ritchie JM, Wilkie DR. The dynamics of muscular contraction, *The Journal of physiology,* 1958, 143(1): 104-113.

[24] Hasselman CT, Best TM, Seaber AV, Garrett Jr WE. A threshold and continuum of injury during active stretch of rabbit skeletal muscle, *The American Journal of Sports Medicine,* 1995, 23(1): 65–73.

[25] Millard M, Franklin DW, Herzog W. A three filament mechanistic model of musculotendon force and impedance, *bioRxiv,* https://doi.org/10.1101/2023.03.27.534347*,* 2023.

[26] Rode C, Siebert T, Blickhan R. Titin-induced force enhancement and force depression: a 'sticky-spring'mechanism in muscle contractions?, *Journal of theoretical biology,* 2009, 259(2): 350–360.

[27] Schappacher-Tilp G, Leonard T, Desch G, Herzog W. A novel three-filament model of force generation in eccentric contraction of skeletal muscles, *PloS one,* 2015, 10(3): e0117634.

[28] Nishikawa K, Huck TG. Muscle as a tunable material: implications for achieving muscle-like function in robotic prosthetic devices, *Journal of Experimental Biology,* 2021, 224(19): 1-10.

[29] Gordon AM, Huxley AF, Julian FJ. Tension development in highly stretched vertebrate muscle fibres. *The Journal of physiology,* 1966, 184(1): 143–169.

[30] Gordon AM, Huxley AF, Julian FJ. The variation in isometric tension with sarcomere length in vertebrate muscle fibres, *The Journal of Physiology,* 1966, 184(1): 170-192.

[31] Bennett MB, Ker RF, Imery NJ, Alexander RM. Mechanical properties of various mammalian tendons, *Journal of Zoology,* 1986, 209(4): 537-548.

[32] Swammerdam J, The Book of Nature II, 122–132, *Seyffert*, London, United Kingdom*,* 1758.

[33] Maganaris CN, Baltzopoulos V, Ball D, Sargeant AJ. In vivo specific tension of human skeletal muscle, *Journal of applied physiology,* 2001, 90(1): 865–872.

[34] Winters TM, Takahashi M, Lieber RL, Ward SR. Whole muscle length-tension relationships are accurately modeled as scaled sarcomeres in rabbit hindlimb muscles, *Journal of Biomechanics,* 2011, 44(1): 109–115.

[35] Rome LC, Sosnicki AA, Goble DO. Maximum velocity of shortening of three fibre types from horse soleus muscle: implications for scaling with body size, *The Journal of Physiology,* 1990, 431(1): 173–185.

[36] Herzog JA, Leonard TR, Jinha A, Herzog W. Are titin properties reflected in single myofibrils?, *Journal of biomechanics,* 2012, 45(11): 1893–1899.

[37] Prado LG, Makarenko I, Andresen C, Krüger M, Opitz CA, Linke WA. Isoform diversity of giant proteins in relation to passive and active contractile properties of rabbit skeletal muscles, *The Journal of general physiology,* 2005, 126(5): 461–480.

[38] Scott SH, Brown IE, Loeb GE. Mechanics of feline soleus: I. Effect of fascicle length and velocity on force output, *Journal of Muscle Research & Cell Motility,* 1996, 17: 207–219.

[39] Scott SH, Loeb GE. Mechanical properties of aponeurosis and tendon of the cat soleus muscle during whole-muscle isometric contractions, *Journal of Morphology,* 1995, 224(1): 73–86.

[40] Sun JS, Tsuang YH, Liu TK, Hang YS, Cheng CK. Failure sites and peak tensile forces of the composite triceps surae muscle by passive extension in the rabbit, *Clinical Biomechanics,* 1994, 9(5): 310–314.

[41] Siebert T, Rode C, Herzog W, Till O, Blickhan R. Nonlinearities make a difference: comparison of two common Hill-type models with real muscle, *Biological cybernetics,* 2008, 98: 133–143.

[42] Granzier H, Kellermayer M, Helmes M, Trombitás K. Titin elasticity and mechanism of passive force development in rat cardiac myocytes probed by thin-filament extraction, *Biophysical Journal,* 1997, 73(4): 2043–2053.

[43] Noonan TJ, Best TM, Seaber AV, Garrett Jr WE. Identification of a threshold for skeletal muscle injury, *The American journal of sports medicine,* 1994, 22(2): 257–261.

[44] Correia MA, McLachlin SD, Cronin DS. Vestibulocollic and cervicocollic muscle reflexes in a finite element neck model during multidirectional impacts, *Annals of Biomedical Engineering,* 2021, 49(7): 1645–1656.

[45] Happee R, de Bruijn E, Forbes PA, van der Helm FCT. Dynamic head-neck stabilization and modulation with perturbation bandwidth investigated using a multisegment neuromuscular model, *Journal of biomechanics,* 2017, 58: 203–211.

[46] Östh J, Brolin K, Carlsson S, Wismans J, Davidsson J. The occupant response to autonomous braking: a modeling approach that accounts for active musculature, *Traffic injury prevention,* 2012, 13(3): 265–277.

[47] Putra IPA, Iraeus J, Sato F, Svensson MY, Linder A, Thomson R. Optimization of female head–neck model with active reflexive cervical muscles in low severity rear impact collisions, *Annals of biomedical engineering,* 2021, 49: 115–128.

[48] Wochner I, Nölle LV, Martynenko OV, Schmitt S. 'Falling heads': investigating reflexive responses to head–neck perturbations, *BioMedical Engineering OnLine,* 2022, 21(1): 1-23.

[49] Scataglini S, Paul G, editors. DHM and Posturography, 243-260, Academic Press, London, United Kingdom, 2019.

[50] Sacks RD, Roy RR. Architecture of the hind limb muscles of cats: functional significance, *Journal of Morphology,* 1982, 173(2): 185–195.

[51] Netti P, D'amore A, Ronca D, Ambrosio L, Nicolais L. Structure-mechanical properties relationship of natural tendons and ligaments, *Journal of Materials Science: Materials in Medicine,* 1996, 7: 525–530.

APPENDIX A

Table 1: Architectural properties of the MAT_156 and the VEXAT cat soleus models used to simulate Herzog and Leonard [9]. The values for ℓ_o^M and f_o^M differ in the direction of the CE to accommodate for the VEXAT's pennation model: the values of ℓ_o^M and f_o^M are identical when evaluated along the VEXAT's tendon.

Parameter	Symbol	MAT_156	VEXAT	Source
Optimal CE Length	ℓ_o^M	42.5 mm	42.9 mm	[9]
Pennation Angle	α	0°	7°	[50]
Max. Isometric Force	f_o^M	21.6 N	21.8 N	[9]
Max. Shortening Vel.	v_{MAX}^M	4.5 ℓ_o^M /s	4.5 ℓ_o^M /s	[38]
Tendon Slack Length	ℓ_s^T	30.5 mm	30.5 mm	[39] [9]
Tendon Stiffness	k_o^T	(rigid)	30 f_o^M /ℓ_s^T	[39]
Norm. Tendon Damping	U	(rigid)	0.057 1/s	[51]
ECM Fraction	P	-	56%	[37]